Atmos. Chem. Phys. Discuss., doi:10.5194/acp-2015-1013, 2016
Manuscript under review for journal Atmos. Chem. Phys.
Published: 18 January 2016

Atmospheric Chemistry and Physics Discussions

Using critical area analysis to deconvolute internal and external particle variability in heterogeneous ice nucleation

Hassan Beydoun[1] and Ryan C. Sullivan[1,*]

[1] Center for Atmospheric Particle Studies, Carnegie Mellon University, Pittsburgh PA

Correspondence to: R. C. Sullivan (rsullivan@cmu.edu)

Abstract

Heterogeneous ice nucleation remains one of the outstanding problems in cloud physics and atmospheric science. Experimental challenges in properly simulating particle-induced freezing processes under atmospherically relevant conditions have largely contributed to the absence of a consistent and comprehensive parameterization of immersion freezing properties. Here we formulate an ice active surface site based stochastic model of heterogeneous freezing with the unique feature of invoking a continuum assumption on the ice nucleating activity (contact angle) of an aerosol particle's surface, that requires no assumptions about the size or number of active sites. The result is a particle specific property g that defines a distribution of local ice nucleation rates. Upon integration this yields a full freezing probability function for an ice-nucleating particle.

Current cold plate droplet freezing measurements provide a great resource for studying the freezing properties of many atmospheric aerosol systems. A method based on statistical significance to determine an ice nucleating species' specific critical surface area is presented that can resolve the two-dimensional nature of the ice nucleation ability of aerosol particles: *internal* variability in active site strengths and freezing rates along an individual particle's surface, as well as *external* variability between two particles of the same type in an aerosol population. By applying this method to experimental data we demonstrate its ability to comprehensively interpret immersion freezing temperature spectra of droplets containing variable particle concentrations. It is shown that general active site density functions such as the popular n_s parameterization cannot be reliably extrapolated below this critical area threshold to describe freezing curves for lower particle surface area concentrations. Freezing curves obtained below this threshold

Atmos. Chem. Phys. Discuss., doi:10.5194/acp-2015-1013, 2016
Manuscript under review for journal Atmos. Chem. Phys.
Published: 18 January 2016

Atmospheric Chemistry and Physics Discussions

translate to higher n_s values, while the n_s values are essentially the same from curves obtained above the critical area threshold. However, we can successfully predict the lower concentration freezing curves, which are more atmospherically relevant, through a process of random sampling from the statistically significant global distribution obtained from high particle concentration data. Our analysis further revealed that one individual atmospheric illite mineral particle will not contain the entire range of ice active site activity for that system (its internal variability). Comprehensive parameterizations that can predict the temporal evolution of the frozen fraction of cloud droplets in larger atmospheric models are also derived from this new framework.

1 Introduction

Above water's homogenous freezing temperature near -38 °C supercooled cloud droplets can only crystallize on a rare subset of atmospheric aerosol particles termed ice nucleating particles (INP) (Baker and Peter, 2008; Vali et al., 2015). The scarcity of these particles directly affects cloud structure, evolution, and precipitation via inducing the Wegener–Bergeron–Findeisen (WBF) process, where ice crystals rapidly grow at the expense of liquid cloud droplets in mixed-phase clouds. Ice nucleation thus plays a crucial role in determining cloud evolution, lifetime, and properties, creating important feedbacks between aerosols, clouds, precipitation, and climate (Pruppacher & Klett, 1997; Rosenfeld et al., 2008). As a result, most precipitation over land is induced by cloud glaciation (Cantrell and Heymsfield, 2005; Mülmenstädt et al., 2015). Accurate representation of cirrus and mixed phase clouds in atmospheric models therefore necessitates properly parameterizing the heterogeneous ice nucleation process (DeMott et al., 2010; Eidhammer et al., 2009; Hoose et al., 2010; Liu and Penner, 2005) for different aerosol source types and compositions that possess a wide range of heterogeneous ice nucleation activities (Phillips et al., 2008, 2013).

Great challenges in observing the actual heterogeneous ice nucleation nanoscale process is the main culprit impeding the formulation of a consistent and comprehensive framework that can accurately and efficiently represent heterogeneous ice nucleation in atmospheric models (Cantrell and Heymsfield, 2005); we still do not understand what

Atmos. Chem. Phys. Discuss., doi:10.5194/acp-2015-1013, 2016
Manuscript under review for journal Atmos. Chem. Phys.
Published: 18 January 2016

precisely controls the ice nucleation ability of ice active surface sites that catalyze ice embryo formation. There are currently two competing views on the dominant factors that control the heterogeneous ice nucleation process, the stochastic versus deterministic framework (Niedermeier et al., 2011; Vali, 2014). The stochastic framework assumes that freezing occurs randomly across a particle's surface and can be constrained with a temperature dependent nucleation rate (Pruppacher and Klett, 1997). This effectively yields time dependent freezing and an element of non-repeatability (Vali, 2008). On the other hand in the deterministic framework ice nucleation is dictated by well characterized ice active surface sites (Fletcher, 1969; Meyers et al., 1992). Each active site has a characteristic critical freezing temperature, with the site with the highest critical temperature always initiating crystallization instantly (Vali, 2008). Careful examination of the experimental results published by Vali (2008) indicates that the very nature of the process need not be in contention. These results show that there is a strong spatial preference on where nucleation occurs, supporting the existence of discrete active sites. However, temperature fluctuations still occur indicating that a stochastic element also exists. Considering several decades of experimental work, and theoretical considerations (Ervens and Feingold, 2013; Murray et al., 2012; Vali and Stransbury, 1966; Vali, 1994, 2014; Wright and Petters, 2013; Wright et al., 2013), the role of time has been determined to play a much weaker role than temperature does. It remains to be seen whether the difference is significant enough for time-dependent freezing to be completely in atmospheric models.

The debate over how to properly parameterize heterogeneous ice nucleation has important implications on how freezing processes are represented in atmospheric models (Hoose and Möhler, 2012; Hoose et al., 2010; Koop et al., 2000; Phillips et al., 2008, 2013), and also reflects our fundamental understanding of this nucleation process. Ervens & Feingold (2012) tested different nucleation schemes in an adiabatic parcel model and found that critical cloud features such as the initiation of the WBF process, liquid water content, and ice water content, all diverged for the different parameterizations. This strongly affected cloud properties and lifetime. The divergence was further exaggerated as the system gained complexity – for example by switching the monodisperse ice nucleating particle size distributions to a polydisperse distribution. This indicates that

Atmos. Chem. Phys. Discuss., doi:10.5194/acp-2015-1013, 2016
Manuscript under review for journal Atmos. Chem. Phys.
Published: 18 January 2016

Atmospheric Chemistry and Physics Discussions

with more sophisticated and realistic systems the variations between the modeled results caused by different freezing parameterizations can be even more drastic.

A new parameterization, derived from the first principles of classical nucleation theory, is formulated in this paper. The new framework is stochastic by nature to properly reflect the randomness of ice embryo growth and dissolution, but also accounts for the variable nature of an ice nucleant's surface and the distribution of ice active surface site ability across a particle's surface (internal variability), and between individual particles of the same type (external variability). The formulation is expanded to encompass the variability in surface site activity between different ice nucleating particles in an aerosol population. A new method is presented to analyze and interpret the ubiquitous droplet freezing cold plate experiments using this framework, and parameterize these experimental results for use in cloud parcel models. New insights into the proper design of cold plate experiments and the analysis of their immersion freezing datasets to accurately describe the behavior of atmospheric ice nucleating particles are revealed.

2 Classical nucleation theory

Ice nucleation is a fundamentally stochastic process brought about by the random formation, growth, and dissolution of critically sized ice germs that overcome the energy barrier associated with the phase transition. A homogenous ice nucleation rate for a given volume of supercooled water can therefore be defined from a Boltzmann type formulation:

$$J(T) = Cexp\left(-\frac{\Delta G}{kT}\right) \qquad (1)$$

where J is the ice nucleation rate and has units of freezing events/(time × volume). ΔG is the energy barrier to crystallization from liquid water as defined in Pruppacher & Klett (1997) and Zobrist et al. (2007). T is temperature, k the Boltzmann constant, and C is a constant. For typical cloud droplet volumes, a temperature of about -38 °C is typically required for the homogeneous ice nucleation rate to become significantly fast such that freezing occurs within minutes or less. At temperatures between -38 and 0 °C a catalyst is required to initiate freezing of cloud droplets. Certain rare aerosol particles – ice

Atmos. Chem. Phys. Discuss., doi:10.5194/acp-2015-1013, 2016
Manuscript under review for journal Atmos. Chem. Phys.
Published: 18 January 2016

Atmospheric Chemistry and Physics Discussions

nucleating particles – can act as these catalysts and induce heterogeneous ice nucleation in the atmosphere.

In expanding to heterogeneous ice nucleation the simplest approach is to assume that instead of ice germ formation occurring randomly throughout a bulk volume of supercooled water, ice nucleation is initiated on a surface. The surface reduces the nucleation energy barrier ΔG by a factor f, dependent on the contact angle between liquid water and the material. The contact angle θ [0, π] is actually a proxy for the water-surface interaction system, with smaller values of θ indicating that the surface is a better nucleant. The surface's measured water contact angle cannot actually be simply used to predict its ice nucleation efficiency. The extreme limit of a contact angle of 0° is therefore a perfect ice nucleant, diminishing the energy barrier fully and immediately inducing freezing at the thermodynamic freezing point of water at 0 °C. The heterogeneous ice nucleation rate for a volume of water containing a total surface area of ice nucleating particles (INP) therefore can be defined as (Pruppacher and Klett, 1997):

$$J(T) = Cexp\left(-\frac{f(\theta)\Delta G}{kT}\right) \qquad (2)$$

where J in this case would be expressed as freezing events/(time × surface area).

This pure stochastic formulation (also known as classical nucleation theory (Vali, 2008)) hypothesizes that the nucleation rate is uniform across the ice nucleating particle's surface. For a large statistical ensemble of droplet-INP pairings the number of frozen droplets after some time t resembles a first order chemical decay (Pruppacher and Klett, 1997; Vali, 2008):

$$N_f(T,t) = N(1 - \exp(-J(T)At)) \qquad (3)$$

where N_f is the fraction of droplets frozen after time t at temperature T, N is the total number of particle-droplet pairings and A is the surface area of each individual ice nucleating particle. Furthermore, a probability of ice nucleation, P_f, at the single droplet-particle level can be defined as:

$$P_f = 1 - \exp(-JAt) \qquad (4)$$

Atmos. Chem. Phys. Discuss., doi:10.5194/acp-2015-1013, 2016
Manuscript under review for journal Atmos. Chem. Phys.
Published: 18 January 2016

Atmospheric Chemistry and Physics Discussions

3 Formulation of g: a continuum approach of active site activity to describe heterogeneous ice nucleation

A more realistic approach is to recognize that the heterogonous nucleation rate will vary along the particle-droplet interface given the large variability in particle surface composition and structure across any one particle, which in turn determines the activity (or contact angle, θ) of each discrete ice active surface site. Since the critical nucleation area (~nm^2) is much smaller than the total particle area (~μm^2), we apply a continuum assumption for the ice active site activity (θ) available across a particle's surface without assumptions about the size or number of active sites per particle surface area. The new resulting probability of freezing is:

$$P_f = 1 - \exp(-t \int J \, dA) \qquad (5)$$

where J is now a freezing rate that is allowed to vary for each specific infinitesimally small segment of the particle's surface area, dA. To define the freezing probability as a function of a contact angle distribution, the surface integral (Eq. 5) is transformed into a line integral via the newly defined g parameter and normalized to the total available surface area:

$$g(\theta) = \frac{1}{A}\frac{dA}{d\theta} \qquad (6)$$

and the freezing probability for a droplet-particle pair becomes:

$$P_f = 1 - \exp\left(-tA \int_0^{\pi} J(\theta) g(\theta) d\theta\right) \qquad (7)$$

g is a probability density function describing the continuous active site density of the ice nucleating particle's surface. This is the first use of a continuum description of active site density to our knowledge. Some key unique features of our approach are that the number or size of the individual active sites do not have to be assumed or retrieved in order to predict the freezing probabilities. The causes of these unique features in our framework and the choice of a normal distribution for the contact angle will be explored and justified in a following section.

Atmos. Chem. Phys. Discuss., doi:10.5194/acp-2015-1013, 2016
Manuscript under review for journal Atmos. Chem. Phys.
Published: 18 January 2016

The *internal* variability of an individual ice nucleating particle expresses the heterogeneity of its ice nucleating surface. A wider (larger σ) g distribution describes a greater particle internal variability of ice active surface site properties or contact angles present on that one particle. This is in contrast to the *external* variability of an ice nucleating species, which expresses how diverse a population of particles is in their ice nucleation activities. External variability accounts for differences in the g distributions of individual particles between particles of the same type (such as particles composed of the same mineral phases).

Formulating a heterogeneous ice framework in this manner provides direct insight into the underlying causes of the freezing activity spectrum present in experimentally probed realistic particle systems that possess considerable internal and external variability. In the following sections the model is developed further to shed light on the impact of the g distribution on time dependent freezing, the contrasting internally and externally variable nature of a species' ice nucleating activity, and the complex dependence of g on particle size.

3.1 Internal variability and its impact on time dependent freezing

To explore the importance of accounting for ice nucleating variability along a single particle's surface (internal variability) we examined the temperature dependent freezing curves of droplets with single large ash particles immersed in them from Fornea et al. (2009). Their experiments were performed with cooling rates of 1 °C/min. Figure 1 displays their experimental data (red dots), a single contact angle (θ) fit to their data (red solid line) that assumes no internal variability, and a g distribution fit using multiple θs (solid blue line) that allows for internal variability. Fornea et al. retrieved their experimental data points by averaging the observed freezing temperature of the same ash particle-droplet pair after multiple freezing cycles. The averaged values are denoted freezing probabilities since they represent the chance of freezing occurring at that temperature. The ash particle diameter was around 300 μm, clearly much larger than atmospheric particle sizes.

Atmos. Chem. Phys. Discuss., doi:10.5194/acp-2015-1013, 2016
Manuscript under review for journal Atmos. Chem. Phys.
Published: 18 January 2016

Atmospheric Chemistry and Physics Discussions

To fit a g distribution to an empirical freezing curve, a least square error approach is implemented. A matrix of freezing probabilities is generated for all possible g distributions. If the experimental freezing curve has been retrieved from experiments in which the temperature is dictated by a non-constant cooling rate, an expression that satisfies this condition must be used:

$$P_f = 1 - \exp\left(-A \int_0^t \int_0^\pi J(t,\theta) g(\theta) d\theta dt\right) \qquad (8)$$

In equation (8) J is a function of time because temperature varies with time. If the cooling rate $\dot{T}$ is constant, a simple change of variable can be applied:

$$P_f = 1 - \exp\left(-\frac{A}{\dot{T}} \int_{T_i}^{T_f} \int_0^\pi J(T,\theta) g(\theta) d\theta dT\right) \qquad (9)$$

Equation (9) is therefore used to fit the constant cooling rate dataset from Fornea et al. (2009) considered here as well as datasets considered later in the paper.

The g fit performs much better in capturing the behavior of the observed freezing temperature spectrum in Figure 1, as expected given the greater degrees of freedom allowed for the multiple θ fit. The single θ fit has a steeper dependence on temperature, a natural result of the formulation of classical nucleation theory from the double exponential temperature dependence of the freezing probability in Eq. (4) (J is an exponential function of temperature in itself as can be seen in Eq. (2)) results in an approximately temperature step function. The diversity of nucleating ability on the particle surface captured by the g parameter offsets some of the steepness and yields a more gradual freezing curve, more similar to the actual experimental freezing probability curve. The non-step function nature of the measured freezing probabilities versus T also provides indirect evidence for internal variability in active site ability across one particle – otherwise the droplet-particle pair should freeze every time at the same T.

Two droplet freezing probability fits (dotted lines) are also plotted in Figure 1 under different environmental conditions. Instead of prescribing a cooling rate the freezing probabilities are generated by running Eq. (7) at a constant temperature of 255.5 K with

Atmos. Chem. Phys. Discuss., doi:10.5194/acp-2015-1013, 2016
Manuscript under review for journal Atmos. Chem. Phys.
Published: 18 January 2016

Atmospheric Chemistry and Physics Discussions

each fit for Δt = 1 hour. One fit uses the same g distribution used previously, while the additional single θ fit is approximated as a normal distribution with a near zero standard deviation, similar to a Delta Dirac function. The resultant freezing probabilities are then computed and plotted for constant T. It can be seen that the g fit retains much stronger time dependence, with the freezing probability curve shifting about 5 K warmer and the single θ curve shifting just 1 K warmer after 1 hour.

Wider g distributions therefore yield stronger time dependence due to the partial offset of the strong temperature dependence that classical nucleation theory exhibits. The result emphasizes the importance of accounting for internal variability, as it has consequences on what physical parameters (e.g. time, temperature, cooling rate) can influence the freezing outcome and observed droplet freezing temperature spectrum (Broadley et al., 2012). In Fig. 1 a wider g distribution resulted in higher sensitivity to time, which resulted in a shift of the freezing curve to higher temperatures as the system was allowed to temporally evolve at a fixed temperature.

This significant change in the freezing probability's sensitivity to temperature is the cause of the more gradual rise in the freezing probability for the system when applying a non Delta Dirac g distribution. This is effectively enhancing the stochastic element in the particle's ice nucleation properties. The shallower response of freezing probability to decreasing temperature (deterministic freezing) creates a greater opportunity for time-dependent (stochastic freezing) to manifest, as a larger fraction of the droplets spend more time unfrozen. The enhancement of the stochastic element brings about a more important role for time as shown in Fig. 1.

3.2 Defining g as a normal distribution of ice active site activity

The fit for a particle-freezing curve such as the one considered in the previous section (Fig. 1) does not have a unique solution. There are, mathematically speaking, infinite solutions for the distributions that produce a representative freezing curve. In any considered distribution an ascent in the curve with increasing contact angle represents a competition between more active but less frequent surface sites, and less active but more

Atmos. Chem. Phys. Discuss., doi:10.5194/acp-2015-1013, 2016
Manuscript under review for journal Atmos. Chem. Phys.
Published: 18 January 2016

Atmospheric Chemistry and Physics Discussions

frequent sites. Sites with lower activity and lower frequency have essentially zero chance of contributing to the overall freezing probability, primarily due to the nucleation rate J's exponential dependence on the energy barrier to nucleation and the freezing probability's exponential dependence on J as shown in Eqs. (2) and (7). It is therefore sufficient to conceptualize that the particle has one large effective active site relevant to the ice nucleation process that actually manifests – that causes the particle-droplet system to freeze. This site has a continuum of ice nucleation activity described by the g distribution, as depicted on the upper right hand corner in Fig. 2.

The ascending part of the curve of the normal g distribution covering the smallest (most active) values of θ in Figure 2 can capture this active site model. The wider the defined g distribution (i.e. for a larger standard deviation, σ) the more diverse the considered system is in its internal variability of ice nucleation activity. Simply put the single contact angle description (e.g. red fit line in Fig. 1) is in a way applicable, as long as slight variation around that value of θ is considered to account for the surface diversity of active sites. The variation would encompass the minimum amount of internal variability needed to properly model the freezing behavior of the droplet containing the ice nucleating particle. Since the freezing probability is determined solely by a fraction of the ascent of the normal distribution – as this captures the rare but most active sites that determine the actual freezing rate J and freezing probability P_f – the following approximation to equation (7) can be made:

$$P_f = 1 - \exp\left(-tA\int_0^{\pi} J(\theta)g(\theta)d\theta\right) \approx 1 - \exp\left(-tA\int_{\theta_{c_1}}^{\theta_{c_2}} J(\theta)g(\theta)d\theta\right) \qquad (10)$$

where θ_{c_1} and θ_{c_2} are the approximate cutoff points in the g distribution that contain the critical range of the most active contact angles. Outside $[\theta_{c_1}, \theta_{c_2}]$ the less active contact angles have a negligible contribution to the actual manifested freezing rate and freezing probability.

Figure 2 also shows a sample distribution of active site ability/contact angle discretized into numerical bins, where the height of each bin represents the abundance of that θ across the particle's surface. The area in each column thus represents the total

Atmos. Chem. Phys. Discuss., doi:10.5194/acp-2015-1013, 2016
Manuscript under review for journal Atmos. Chem. Phys.
Published: 18 January 2016

Atmospheric Chemistry and Physics Discussions

surface area with that value of θ. As in Fig. 2's inset the darker colors are used to emphasize more active ice nucleating activity at the smaller contact angles. The curve in Fig. 2 only displays part of the ascent of the g distribution and in particular the critical contact angle range for small θ values, $[\theta_{c_1}, \theta_{c_2}]$.

The critical contact angles are determined numerically by identifying the range $[\theta_{c_1}, \theta_{c_2}]$ that satisfies Eq. (10). Figure 3 illustrates the process of identifying θ_{c2}. The blue curves represent freezing probabilities computed via integrating Eq. (10) from 0 to a variable θ_{c2}. The red curve is the freezing probability computed from integrating across the full θ range. As θ_{c2} is increased the resultant curve (blue) approaches the curve computed from the full θ range (red). For the system studied in Fig. 3, a value of θ_{c2} = 1.1 captures 99.9% of the complete freezing probability found using the full range of θ.

Furthermore the critical contact angle range provides quantitative insight into the nucleating area of the particle – the total active site surface area where nucleation will take place. The nucleation area $A_{nucleation}$ can be estimated as follows:

$$A_{nucleation} = A \int_{\theta_{c_1}}^{\theta_{c_2}} g(\theta) d\theta \qquad (11)$$

For the system analyzed in the previous section it is estimated that $\theta_{c1} \approx 0.4$ rad and $\theta_{c2} \approx 0.79$ rad. Application of Eq. (11) yields a total ice active surface area estimate of 27 nm^2. Classical nucleation theory estimates that the area of a single active site is 6 nm^2 (Lüönd et al., 2010; Marcolli et al., 2007). The estimated total area of nucleation is therefore consistent with this value and supports the argument that competition between sites along the critical range is taking place. However the surface area where ice nucleation is occurring remains a very tiny fraction of the total particle surface.

3.3 Using critical area analysis to predict droplet freezing spectra obtained in cold plate experiments

Experiments in which one particle is immersed in one droplet in a cold plate system provide direct insight into internal and external variability. However analytical challenges

Atmos. Chem. Phys. Discuss., doi:10.5194/acp-2015-1013, 2016
Manuscript under review for journal Atmos. Chem. Phys.
Published: 18 January 2016

Atmospheric Chemistry and Physics Discussions

only allow for individual particles that are on the order of hundreds of microns to be probed in this way. Particles of that enormous size are not atmospherically relevant in the context of heterogeneous ice nucleation (DeMott et al., 2010) and would have very short atmospheric lifetimes versus depositional removal. These large particles may be exaggerating some of the internal variability observed and fit by the g distribution because they provide much larger surface area with potentially more diversity in ice nucleating ability. We present a method for resolving the two dimensional variability – internal and external variability – for cold plate droplet freezing experiments that probe much smaller realistic particle sizes but at the cost of high particle numbers per droplet.

Many droplet freezing array experimental methods such as those described in (2012), Murray et al. (2011), Wright & Petters (2013), and Hiranuma et al. (2015) use atmospherically relevant particle sizes (hundreds of nanometers to a few microns in diameter) but create the droplet array from a prepared suspension of the particles of interest in water. The resultant particle concentrations are typically high and the number of particles present in each droplet has to be approximated using statistical methods. When total particle surface area is high enough it is conceivable that a threshold of statistical significance is reached whereby most of the species' maximum possible external variability is already available within the particle-droplet system. At this point no additional diversity in external variability (ice active site ability or θ) is created by further increasing the total particle surface area in the water volume; the external variability has effectively saturated. Past this surface area threshold each member of the system's population (droplets with particles immersed in them) become approximately identical in their ice nucleation properties and the theoretical frozen fraction can be expressed as:

$$F = P_f(one\ \text{system}) = 1 - \prod_{i=1}^{n} P_{uf,i} \qquad (12)$$

where F is the droplet frozen fraction, n is the number of particles per droplet, and $P_{uf,i}$ is the probability that the system i does not freeze. Further expanding the expression yields:

$$F = 1 - \exp\left[-t\left(\sum_{i=1}^{n} A_i \int_0^{\pi} J(\theta) g_i(\theta) d\theta\right)\right] = 1 - \exp\left[-t \int_0^{\pi} J(\theta) \sum_{i=1}^{n} (A_i g_i) d\theta\right] \qquad (13)$$

Atmos. Chem. Phys. Discuss., doi:10.5194/acp-2015-1013, 2016
Manuscript under review for journal Atmos. Chem. Phys.
Published: 18 January 2016

Next the parameter $\bar{g}$ is defined:

$$\bar{g} = \frac{\sum_{i=1}^{n}(A_i g_i)}{A_t} \qquad (14)$$

where A_t is the sum of all particle surface area available inside a given droplet, and A_i is the surface area representing that value of g_i (which is a function of θ). Equation (13) then becomes:

$$\Rightarrow F = 1 - \exp\left(-tA_t \int_0^{\pi} J(\theta)\overline{g(\theta)}d\theta\right) \qquad (15)$$

$\bar{g}$ is the arithmetic average of all the g distributions for a statistically significant ensemble of particles in the droplet (each particle has its own g distribution). Alternatively $\bar{g}$ can be thought of as the probability density function for all possible ice nucleating activity of a given species or particle type. It is worth mentioning that $\bar{g}$ is a true continuous probability density function. While the g distribution of an individual particle is an approximate continuous function – due to the very small size of ice nucleating active sites – $\bar{g}$ contains all possible values of contact angles that an ice nucleating species can exhibit.

Above a certain surface area threshold the probability of an ice-nucleating particle surface not possessing the entire range of ice nucleating activity (θ) becomes very small. This threshold surface area will be referred to as the critical area. Any particle or ensemble of particles having a total surface area larger than the critical area can be reliably approximated as having $\bar{g}$ describe the actual g distribution of the individual particles. In other words, for large particles with more surface area than the critical area threshold, the external variability between individual particles will be very small such that the particle population can just be described by one average continuous distribution of the ice active site ability.

To resolve the g distributions of the systems possessing particle surface areas smaller than the critical area the first step is to determine this threshold of statistical significance. Experiments must start at very high particle surface area concentrations to ensure the number of particles and total surface area per droplet exceeds statistical significance. For the case study considered next for example, high particle concentrations were those that

Atmos. Chem. Phys. Discuss., doi:10.5194/acp-2015-1013, 2016
Manuscript under review for journal Atmos. Chem. Phys.
Published: 18 January 2016

Atmospheric Chemistry and Physics Discussions

resulted in total particle surface areas greater than about 2.02×10^{-6} cm^2. The particle number or surface area concentration is then decreased until the retrieved averaged g distribution (from the measured droplet freezing temperature spectrum for an array of droplets containing particles) significantly diverges from $\bar{g}$. This point can identify the parameter A_c, the critical area of the species under study. A schematic of the procedure is summarized in Fig. 4.

Figure 4 also plots the popular exclusively deterministic scheme's ice active site density parameter n_s (Vali, (2008), Murray et al. (2011), Broadley et al. (2012), Hiranuma et al. (2015), and Wex et al. (2015), amongst others), retrieved directly from freezing curves of droplets with illite particles immersed in them measured in a cold plate system by Broadley et al. (2012) and used to produce the right panel in Fig. 4. Similar to $\bar{g}$, n_s assumes active site diversity can be defined independently of the surface area (it is multiplied by total surface area to estimate total heterogeneous ice nucleation activity). As the total particle surface area of the system under study is reduced from the blue to the red curve, the retrieved n_s values are similar indicating that variability of active sites remains constrained within droplets. Note that both the red and blue curves were obtained from systems we have determined were above the critical area threshold. Further reduction of total surface area to below the critical area threshold shifts the n_s values noticeably, as seen by the significant increase in n_s(T) for the green curve. As all three curves were obtained by just varying the particle concentration of the same species the same n_s values should be retrieved for all three curves; the n_s scheme is designed to normalize for the total surface area or particle mass present. This is successful for the higher particle surface area systems (red and blue curves are similar) but not at lower particle area (green curve diverges). The large increase in n_s observed when total surface area is below the critical area threshold indicates that the observed droplet freezing temperature spectra do not just linearly scale with particle concentration or surface area. Further analysis will show this is not due to an enhancement of ice nucleating activity per surface area but is actually a product of external variability causing a broadening of the ice nucleating spectrum within the droplet ensemble when total surface area is below the critical area threshold. The curves plotted in Fig. 4 were derived using experimental cold plate droplet freezing data for illite mineral particles presented by Broadley et al. (2012)

Atmos. Chem. Phys. Discuss., doi:10.5194/acp-2015-1013, 2016
Manuscript under review for journal Atmos. Chem. Phys.
Published: 18 January 2016

Atmospheric Chemistry and Physics Discussions

as we discuss further below. We have observed other similarly large effects of particle concentration on the measured droplet freezing temperature spectrum and the retrieved n_s curves from our own cold plate measurements. This includes droplet freezing measurements of mineral systems such as illite, as well as Snomax bacterial particles, and cellulose particles.

To predict the freezing curves of the droplets with particle surface areas lower than the estimated critical area, the aggregate surface area of the entire particle population within each droplet is modeled as one large surface. A contact angle θ_r is randomly selected and the value of the g distribution for the particle being sampled for at θ_r is assigned the value of $\overline{g(\theta_r)}$:

$$g_p(\theta_r) = \overline{g(\theta_r)} \qquad (16)$$

This process is repeated for a parameter n_{draws} and for the number of droplets that produce the freezing curve being modeled. n_{draws} is the only parameter that is optimized for so the modeled freezing curves can predict the behavior of the experimental freezing curves. The sampled g distributions are normalized with respect to the estimated total surface area for the system being modeled before being used to compute the freezing probability. Using the sampled g distributions the freezing probability of each droplet is calculated using Eq. (9) and the frozen fraction curve is computed from the arithmetic average of the freezing probabilities:

$$F(below\ critical\ area) = \frac{1}{N}\sum_{i=1}^{N} P_{f_i} \qquad (17)$$

where N is the number of droplets in the cold plate array.

The method is applied to freezing curves measured for decreasing particle concentrations by Broadley et al. (2012) for micron sized illite mineral powder particles immersed in droplets and frozen on a cold plate. The authors identified two total surface area regimes by analyzing their droplet freezing curves. In the lower surface area regime they observed a different freezing dependence to particle surface area than at higher surface areas. At higher surface areas they saw no dependence of the freezing curves on total particle surface area, which is inconsistent with both the stochastic and deterministic

Atmos. Chem. Phys. Discuss., doi:10.5194/acp-2015-1013, 2016
Manuscript under review for journal Atmos. Chem. Phys.
Published: 18 January 2016

Atmospheric Chemistry and Physics Discussions

frameworks. For larger droplets the transition seemed to occur at higher total particle surface indicating that there might be a particle concentration effect impacting the total particle surface area per droplet. At lower surface areas/concentrations the authors found the surface area dependence to be consistent with the n_s framework. The factor of almost two difference in n_s values shown in Fig. 4 however has large implications on the freezing temperature curves and droplet freezing temperatures. We argue here that the n_s framework fails to account for changes in total particle surface area present below a critical area threshold.

Figure 5 shows experimental freezing curves (open symbols) all taken from Broadley et al. (2012), with different particle surface area concentrations. The curves from the highest particle concentration experiments, 7.42×10^{-6} (6b) and 2.02×10^{-6} cm^2 (6a), are used to confirm statistical significance by first fitting the 6b curve with a g distribution and then successfully predicting the 6a curve with the same g distribution obtained from 6b and applying a particle surface area correction. This g distribution is therefore assumed to be the $\bar{g}$ of the considered system, since external variability has saturated. Note that above the threshold concentration A_c, a change in the total available surface area A is all that is required to account for how the change in particle concentration shifts the droplet freezing temperature curve. This is not the case when total area is less than the critical area, and what follows is a method to predict these low particle concentration-freezing curves.

Moving to the lower concentration freezing curves (1.04×10^{-6} cm^2 and 7.11×10^{-7} cm^2) the transition to below the statistically significant critical area begins to take place. The solid lines attempt to predict the experimental data points using $\bar{g}$. Predicting experimental data points for the 1.04×10^{-6} cm^2 system with the same statistically significant $\bar{g}$ distribution captures the 50% frozen fraction point but fails at accounting for the broadness on the two ends of the temperature measurements. The statistically significant prediction ($\bar{g}$) completely deteriorates in quality for the lowest concentration experiments (7.11×10^{-7} cm^2) as it neither captures the shape nor the 50% frozen fraction point. If however the described numerical model is used, in which random sampling from the ice nucleating spectrum dictated by $\bar{g}$ is carried out to predict a freezing curve, the

Atmos. Chem. Phys. Discuss., doi:10.5194/acp-2015-1013, 2016
Manuscript under review for journal Atmos. Chem. Phys.
Published: 18 January 2016

Atmospheric Chemistry and Physics Discussions

behavior of the experimental curve is both qualitatively and quantitatively captured. The dotted lines are obtained by sampling from the $\bar{g}$ model to successfully predict the behavior of all the freezing curves. The early freezing onsets of the lower concentration systems are captured with the model as well as the broadness in the curves. After $\bar{g}$ was obtained from the high concentration data above the critical area threshold, the only parameter that had to be optimized to produce these accurate predicted freezing curves was n_{draws}. This optimization of n_{draws} can be omitted if a computationally expensive brute force calculation is applied where each particle surface is partitioned into small 1 nm^2 unit areas and random θ assignments are carried out for each.

One notable characteristic is how these curves ascend together with decreasing temperature but then diverge as the temperature decreases further. The closeness of the data at warmer temperatures (the ascent) is interpreted as the presence of some rare high activity active sites within the particle population under all the particle concentrations explored in their experiments. As the single most efficient active site causes the entire droplet to freeze, so long as there is one such site in each droplet the same freezing temperature will be observed. At lower temperatures it appears that there is a wider diversity in the activity of droplets that did not contain these rare efficient active sites, and thus there is significant spread in the freezing curve for T < 242 K. This is probably due to strong external variability of the ice nucleating population, with very strong/active nucleators causing similar freezing onsets for different particle concentrations at the warmer temperatures, and a lack of strong nucleators explaining the less consistent freezing of the unfrozen droplets at lower temperature. The droplets that freeze at lower temperatures are the "leftover" droplets that did not contain at least one very active surface site. Thus it makes sense that there is a wider spread in the freezing curves for these droplets, as their freezing temperature is highly sensitive to the presence of moderately strong active sites. This expresses a greater diversity in external variability – the active site activity possessed by individual particles from the same particle source. In a later section the claim of more external variability contributing to the broader curves below the statistically significant threshold is supported with a closer look at the numerical results from the model.

Atmos. Chem. Phys. Discuss., doi:10.5194/acp-2015-1013, 2016
Manuscript under review for journal Atmos. Chem. Phys.
Published: 18 January 2016

Atmospheric Chemistry and Physics Discussions

3.4 Comparison between, $\bar{g}$, n_s, and other existing parameterizations of heterogeneous ice nucleation

This is the first heterogeneous ice nucleation parameterization that resolves the two-dimensional active site internal and external variability of particle samples probed experimentally. The popular exclusively deterministic scheme (Broadley et al., 2012; Murray et al., 2012; Vali, 1994, 2008; amongst others) prescribes an ice active site density function n_s that is an intensive property of the species under study. The frozen fraction of the ensemble is computed from a time independent equation:

$$F = 1 - \exp(-n_s(T)A) \qquad (18)$$

Equations (15) and (18) have a very close mathematical form. Both carry a negative exponential dependence on surface area, and temperature dependence in the rest of the variables is inside the exponential.

Fitting freezing curves below the statistically significant threshold with n_s yields errors similar to fitting the curves with $\bar{g}$. Doing so has an inherent assumption of the ice nucleation activity being totally internally variable. This is clear in comparing Eqs. (15) and (18). That is $\bar{g}$ and n_s both offer incomplete information about the distribution of ice nucleation activity for a species. A similar conclusion along these lines was reached by Broadley et al. (2012) when the authors noted that the best fits to their freezing curves were achieved when the system was assumed to be totally externally variable. They found explicit active site distributions for each freezing curve however and did not generate predictions from a more general (global) statistically significant active site distribution as we have done here.

There are other formulations that hypothesize a multi-component stochastic model such as the ones described in Vali & Stransbury (1966), Niedermeier et al. (2011), Wheeler and Bertram (2012), and Wright and Petters (2013). Vali and Stranbury (1966) were the first to recognize that ice nucleating surfaces are diverse and stochastic and thus active sites need to be assigned both a characteristic freezing temperature as well as fluctuations around that temperature. Niedermerier et al. (2011) proposed the soccer ball

Atmos. Chem. Phys. Discuss., doi:10.5194/acp-2015-1013, 2016
Manuscript under review for journal Atmos. Chem. Phys.
Published: 18 January 2016

Atmospheric Chemistry and Physics Discussions

model, in which a surface is partitioned into discrete active sites with each site conforming to classical nucleating theory. Marcolli et al. (2007) found a Gaussian distribution of contact angles could best describe their heterogeneous ice nucleation data in a completely deterministic framework. Wright and Petters (2013) hypothesized the existence of a Gaussian probability density function for a specific species, which in essence is similar to the $\bar{g}$ framework described here. However no distinction between curves below and above a critical threshold of total surface area was made as active site distributions sampled from the general distribution were generated to fit their freezing curves. This required optimizing for the hypothesized Gaussian distribution using all freezing curves, and not independently fitting high concentration freezing curves. Their method also required making assumptions about the size of the active site, a parameter that does not necessarily need to be defined if the critical range of θ is carefully investigated as we have done here.

Multi-component stochastic formulations have thus far failed to become a standard for experimentalists to interpret their data with, while n_s is now commonly used to describe cold plate and other droplet freezing experimental data (Hiranuma et al., 2015; Murray et al., 2012; Wex et al., 2015). This is in part due to the necessary inclusion of more variables required by other frameworks (such as prescribing a discrete number of active sites as described in Niedermeier et al. (2011)) than the simpler purely deterministic scheme of n_s. The new formulation described here requires only prescribing a species' heterogeneous ice nucleation ability as a function $\bar{g}$ along with finding the critical area A_c. The critical area is determined by repeatedly measuring freezing curves for the same system or sample using different particle concentrations. Varying particle concentration is already routinely used in cold plate experiments to widen the droplet freezing temperature range that can be measured. An estimate of the total surface area of the particles under study must be made and associated with the retrieved freezing curves. While a process of random sampling is initially necessary for determining the behavior below the critical area, in a following section we will introduce easy to apply parameterizations that can be used to replace the recurrent use of this computationally cumbersome process.

Atmos. Chem. Phys. Discuss., doi:10.5194/acp-2015-1013, 2016
Manuscript under review for journal Atmos. Chem. Phys.
Published: 18 January 2016

Atmospheric Chemistry and Physics Discussions

3.5 Dependence of g on ice nucleating particle size

The particle size dependence of the freezing probability comes from the exponential dependence of the freezing probability on the surface area A as shown in Eq. (7). The freezing probability's sensitivity to surface area is the same as its sensitivity to time however the quadratic dependence of area on radius makes size a more sensitive parameter than time. Furthermore there might be more subtle size dependencies in the g function itself. For a given particle type, whether size affects the diversity (internal variability) of nucleating sites is not something that can be trivially probed experimentally. To accurately test any potential size dependence, particles of varying sizes need to be probed individually and compared. Measurements in which particles were size selected before assessing their ice nucleation ability have been performed, such as those using continuous flow diffusion chambers as described in Koehler et al. (2010), Lüönd et al. (2010), Sullivan et al. (2010a), Welti et al. (2009), among others. However, a similar limitation to the cold plate experiments presents itself in which the freezing onsets of many droplets containing a range of particle sizes are averaged to find a frozen fraction curve. The resultant curves have potential internal and external variability embedded, with not enough information to disentangle them.

The argument for the existence of a species' specific critical area can be made for either a total number of particles in a specific size range or a total particle surface area. Assuming that a single species' surface area does not undergo intensive changes in its ice nucleation properties (such as chemical processing as discussed in Sullivan et al. (2010a, 2010b)) a cut off statistically significant size can be defined. Above this critical size the active site distribution is $\bar{g}$ while below it is some distribution of g's that can be sampled from $\bar{g}$. In the case study considered here in Fig. 5 for illite mineral particles the criticalf surface area was around 10^{-6} cm^2. This corresponds to a single spherical particle with an equivalent diameter of around 10 μm, a size cutoff that is quite atmospherically relevant (DeMott et al., 2010). The vast majority of the atmospheric particle number and surface area distributions are found at sizes smaller than 10 μm. Thus we conclude that for illite mineral particles, individual atmospheric particles will not contain the entire range of ice

Atmos. Chem. Phys. Discuss., doi:10.5194/acp-2015-1013, 2016
Manuscript under review for journal Atmos. Chem. Phys.
Published: 18 January 2016

Atmospheric Chemistry and Physics Discussions

active site activity ($\bar{g}$) within that one particle, and each particle's ice nucleation ability is best described by an individual g distribution (that is a sub-sample of $\bar{g}$).

Application of Eq. (11) to find $A_{nucleation}$ for illite systems 6a (2.02×10^{-6} cm^2) and 5a (1.04×10^{-6} cm^2) from Broadley et al. (2012) gives insight into how the nucleating area is influencing the shape of the freezing curves. System 6a is where the critical area cutoff was found to occur while 5a started to exhibit the behavior of a broader freezing curve with a similar onset of freezing but with a diverging tail, indicating it is below the critical surface area. In Fig. 6 the average cumulative ice nucleating area computed from Eq. (11) is plotted against the critical contact angle range for the two systems. The total nucleating area at low contact angles is strikingly close between the two systems. This is because statistically the chance of possessing rare and highly active sites in an ensemble as large as system 5a is high as these occupy a small portion of the total particle area but have a substantial impact on the freezing behavior. This explains why the onset of freezing for the two curves is so similar. The diverging tail can be attributed to the divergence of the nucleating areas at higher contact angles in the critical contact angle range. The steeper rise of the average nucleating area of system 6a is due to its higher chance of possessing moderately strong active sites compared to system 5a due to the larger surface area present in 6a. This creates a larger spread in the freezing onset of droplets in system 5a after a few droplets initiated freezing in a similar manner to system 6a.

The implications of this analysis on the size dependence of g is that below the critical surface area particles may or may not possess freezing behavior similar to the particles above the critical area threshold. The broadness of the freezing curves 4a and 5a in Fig. 5 is explained by the heterogeneity in ice nucleating ability between the different particles (external variability) and not due to the internal variability within the individual particles themselves. While the broadness of the curves above the critical surface area can be attributed to internal variability, the additional broadness in curves below the critical area cutoff are a result of external variability.

More detailed analysis studying various atmospherically relevant ice nucleating particles needs to be done to shed light on where the statistically significant size cutoff lies for most species. This has important implications on whether one active site density

Atmos. Chem. Phys. Discuss., doi:10.5194/acp-2015-1013, 2016
Manuscript under review for journal Atmos. Chem. Phys.
Published: 18 January 2016

Atmospheric Chemistry and Physics Discussions

function (i.e. $\bar{g}$ or n_s) is sufficient to accurately represent the species' ice nucleating properties in larger cloud or atmospheric models. If not, a more detailed parameterization resolving the multi-dimensional variability may be necessary, such as a series of g or $\bar{g}$ distributions. For illite it seems that external variability is dominant and thus one active site distribution or n_s parameterization does not properly represent the species' ice nucleation behavior. However, if a system's global $\bar{g}$ distribution is obtained then its full ice nucleation behavior is contained within and can be subsampled from $\bar{g}$. Cold plate measurements thus remain a crucial tool for unraveling the complex behavior of ice nucleating material, particularly when a large particle concentration range is probed.

Cold plate experimental data potentially provides sufficient information to describe heterogeneous ice nucleation properties in cloud parcel and atmospheric models, but it is a more involved process then retrieving one active site density (i.e. n_s) parameterization and applying it unconditionally. When samples are investigated, probing a wide concentration range allows determining both general active site density functions (e.g. $\bar{g}$) as well as the behavior of the species' under study at concentrations below the critical area threshold. Once this analysis is undertaken more comprehensive parameterizations can be retrieved as will be developed in the next section.

The critical area analysis carried out in this paper emphasizes the dangers in extrapolating the freezing behavior of droplets containing a large concentration of particle to droplets containing smaller concentrations. Applying a parameterization such as n_s directly to systems below the critical area threshold in a cloud parcel model for example yields large differences in the predictions of the freezing outcome of the droplet population. As the concentration of the species within the droplet was decreased by Broadley et al. (2012), the actual freezing temperature curves diverged more and more from those predicted when the systems were assumed to be above the critical area. This led to significant changes in the retrieved n_s values, as shown in Figure 4. While a less than a factor of 2 change in n_s may seem insignificant, this does have significant effects on the predicted droplet freezing temperature given the exponential dependence of Eq. (18). The large effects of concentration on the droplet freezing temperature can be directly observed in the experimental data from Broadley et al. (2012) plotted in Fig. 5

Atmos. Chem. Phys. Discuss., doi:10.5194/acp-2015-1013, 2016
Manuscript under review for journal Atmos. Chem. Phys.
Published: 18 January 2016

where such a difference in n_s values yielded freezing curves spanning a broader temperature range and a different 50% frozen fraction point. Therefore a cloud parcel model would be unable to accurately predict the freezing onset or the temperature range over which freezing occurs using a single n_s curve obtained from high concentration data. This has huge consequences on the microphysical evolution of the cloud system under study such as the initiation of the Wegener–Bergeron–Findeisen and the consequent glaciation and precipitation rates (Ervens and Feingold, 2012; Ervens et al., 2011).

Systems that probe populations of droplets each containing one particle such as the CFDC are unable to probe a large particles-in-droplet concentration range but are powerful tools for the real-time investigations of ice nucleating particles at the realistic individual particle level (DeMott et al., 2010; Sullivan et al., 2010a; Welti et al., 2009). The frozen fraction curves produced from such an instrument do not provide enough information to associate the observed variability in ice nucleation ability to internal or external factors. However, future laboratory studies using the critical area-cold plate technique we have introduced here (e.g. Fig. 4) will provide new insight into the critical area thresholds of internal variability in ice active site ability for different species. This will produce more informed assumptions regarding the variability in ice nucleation properties observed through online field instruments, specifically when the measurements are made in conjunction with single particle chemical analysis techniques (Creamean et al., 2013; DeMott et al., 2003, 2010; Prather et al., 2013; Worringen et al., 2015).

3.6 Implications of external variability on time dependence

As discussed earlier, time dependence or cooling rate dependence of heterogeneous ice nucleation is affected by the internal variability of the ice active sites across the particle surface area within a droplet. More internal variability reduces the temperature dependence and the role of time potentially grows as a result. Therefore broader freezing curves that derive their broadness from internal variability will be more sensitive to a change in time or cooling rate. While the freezing curves below the critical surface area threshold span a broader temperature range, it is argued that this broadness stems from external variability. The freezing curves below the critical area cutoff are, as depicted in

Atmos. Chem. Phys. Discuss., doi:10.5194/acp-2015-1013, 2016
Manuscript under review for journal Atmos. Chem. Phys.
Published: 18 January 2016

Eq. (17), averages of the freezing curves of the individual droplets. The time or cooling rate dependence therefore is informed by the broadness of the individual droplet freezing curves and not by that of the ensemble.

Broadley et al. (2012) found a nearly non-existent cooling rate dependence of the freezing temperature of droplets containing particle surface areas that have been identified here as falling below the critical area threshold. For four systems with very close estimated total particle surface per droplet, all freezing curves fell within 1 K at the temperature where 50% of the droplets froze, $T_{50\%}$, for a cooling rate range of 1-5 K/min. While our modeled systems below the critical area cutoff did not exhibit zero cooling rate dependence they were slightly less sensitive to the considered cooling rate range than if modeled as totally internally variable (or above the critical area cutoff). The resultant $\Delta T_{50\%}$ for system 4a (7.11×10^{-7} cm^2) is 1.2 K for the totally internally variable system above the critical threshold, and 1.7 K for the system modeled as falling below the critical area cutoff where both internal and external variability are expressed.

4 Application of the g parameterization to cloud models

Particle type-specific $\bar{g}$ distributions and critical areas can be used in larger cloud and atmospheric models to predict freezing onset and the rate of continued ice formation. The simplest parameterization is one that calculates the frozen fraction of droplets, F, for an atmospherically realistic system in which one ice nucleating particle is present in each supercooled droplet, the aerosol particle distribution is monodisperse (all particles therefore have the same surface area A), there is only one species present (therefore use one $\bar{g}$ distribution), and the surface area of the individual particles is larger than that species' critical area. In this case Eq. (14) can be used:

$$F = 1 - exp\left(-tA\int_0^{\pi} J(\theta,T)\overline{g(\theta)}d\theta\right) \qquad (14)$$

If the surface area of the individual particles is smaller than the critical area a modified version of Eq. (14) can be used instead:

Atmos. Chem. Phys. Discuss., doi:10.5194/acp-2015-1013, 2016
Manuscript under review for journal Atmos. Chem. Phys.
Published: 18 January 2016

Atmospheric Chemistry and Physics Discussions

$$F = 1 - exp\left(-tA_c \int_0^{\pi} \left(J(\theta,T)\overline{g(\theta)}d\theta\right)h(A,T)\right) \quad (19)$$

where $h(A,T)$ is an empirically derived parameterization that corrects for the individual particle surface areas of the considered monodisperse aerosol population being smaller than the critical area. Therefore $h(A_c,T) = 1$.

An example of retrieving values of $h(A,T)$ would be in correcting the solid line for system 4a (7.11×10^{-6} cm^2) to the dotted line in Fig. 5. The solid line is the basic use of Eq. (14) however it was shown that the considered experimentally retrieved freezing spectrum was below the critical area threshold. By taking the ratio of the dotted and solid lines values of h can be retrieved for that surface area at each temperature point.

If the aerosol particle population is polydisperse and its size distribution can be expressed as a function of surface area, the frozen fraction can be written as:

$$F = \int_{A_i}^{A_f} \left[1 - \exp\left(-tA \int_0^{\pi} \left(J(\theta,T)\overline{g(\theta)}d\theta\right)h(A,T)dA\right)\right] \quad (20)$$

where A_i and A_f are the minimum and maximum values of the surface areas of the aerosol particle distribution.

If the aerosol ice nucleating population is composed of multiple species, two $\bar{g}$ parameterizations can be formulated for the two cases of an internally mixed (every particle is composed of all the different species) and externally mixed (every particle is composed of just one species). For the case of an internally mixed system Eqs. (14), (19), and (20) can be applied with a $\bar{g}$ distribution that is the surface area weighted average of the $\bar{g}$ distributions of all the considered species. This can be expressed as:

$$\bar{g}_{average} = \frac{1}{A}\sum_{i=1}^{m} A_i \bar{g}_i \quad (21)$$

where A_i is the surface area of the species i, $\bar{g}_i$ is the $\bar{g}$ distribution of the species i, and m is the total number of species. If the system is externally mixed, the frozen fraction can be expressed as:

Atmos. Chem. Phys. Discuss., doi:10.5194/acp-2015-1013, 2016
Manuscript under review for journal Atmos. Chem. Phys.
Published: 18 January 2016

$$F = \frac{1}{m}\sum_{i=1}^{m} F_i \qquad (22)$$

where F_i is the frozen fraction of droplets containing particles of species i and can be retrieved from Eq. (19) or (20).

5 Conclusions

An ice active surface site-based stochastic model of heterogeneous ice nucleation with the unique feature of invoking a continuum assumption on the ice nucleating activity of a particle's surface was formulated. A particle specific property g that defines a distribution of local ice nucleation rates was then derived from the formulation. g is a Gaussian distribution of ice active site activity (contact angle, θ). By analyzing single particle-droplet cold plate freezing spectra, it was shown that internal variability of ice active site activity across a particle's surface can be a significant feature of a particle's observed ice nucleating ability. In addition to impacting the shape of a system's freezing temperature curve, internal variability can also affect a droplet's freezing sensitivity to time. A decrease in internal variability of active site ability, which can be caused by reducing particle-in-droplet concentrations, reduces the sensitivity of the freezing curve to time. Whether this impact is significant enough to merit the exclusion of stochastic effects in cloud and atmospheric models remains to be explored further.

Published cold plate droplet freezing spectra were carefully examined in an attempt to disentangle the internal and external variability contributing to the shapes of the retrieved freezing temperature curves. A method based on the notion of a statistically significant critical total particle surface area threshold was presented. It is argued that a species' entire ice nucleating spectrum can be confined within a global probability density function $\bar{g}$. For a system, be it one particle or an ensemble of particles, to have a total surface area greater than the critical area is a question of whether the surface is large enough to express all the variability in that particle species' ice active surface site ability. By analyzing a case study on illite mineral particles from Broadley et al. (2012) it was shown that freezing curves above a certain critical surface area threshold can be

Atmos. Chem. Phys. Discuss., doi:10.5194/acp-2015-1013, 2016
Manuscript under review for journal Atmos. Chem. Phys.
Published: 18 January 2016

accurately predicted directly from the global $\bar{g}$ distribution obtained from the high particle concentration data alone. The lower particle concentration freezing curves were accurately predicted by randomly sampling active site abilities (θ) from $\bar{g}$ and averaging their resultant freezing probabilities. This framework provides a new method for extrapolating droplet freezing temperature spectra from cold plate experimental data under high particle concentrations to atmospherically realistic dilute particle-droplet systems.

We found that the shifts to colder freezing temperatures caused by reducing the particle concentration or total surface area present in droplets cannot be fully accounted for by simply normalizing to the available surface area, as is done in the ice active site density (n_s) analysis framework. When the surface area is below the critical area threshold the retrieved values of n_s can increase significantly for the same particle species when the particle concentration is decreased. Above the critical area threshold the same n_s curves are retrieved when particle concentration is changed. Atmospheric cloud droplets typically contain just one particle each. Therefore this effect of particle concentration on droplet freezing temperature spectra and the retrieved n_s values has important implications for the extrapolation of cold plate droplet freezing measurements to describe the ice nucleation properties of realistic atmospheric particles.

Atmospherically relevant particle sizes may very well fall below the statistically significant critical area threshold for an individual particle, at least for some species such as illite mineral particles considered here. Therefore average ice nucleation spectra or active site distributions such as n_s and $\bar{g}$ may not be applicable for representing the ice nucleation properties of particles in cloud and atmospheric models. A better representation is a distribution g that is retrieved from a random sampling procedure from the statistically significant global probability distribution function, $\bar{g}$. However to save large-scale models from the cost of generating these distributions for every particle, numerically retrieved correction factors denoted $h(A,T)$ can be used to transform the freezing curve of an ensemble of particle-droplet pairings obtained at particle concentrations above the critical area to atmospherically relevant low particle concentrations below this critical area.

Acknowledgements

This research was partially supported by the National Science Foundation (Award CHE-1213718). The authors thank Dr. Paul DeMott for valuable discussions regarding an earlier version of this framework.

6 References

Andreae, M. O. and Rosenfeld, D.: Aerosol–cloud–precipitation interactions. Part 1. The nature and sources of cloud-active aerosols, Earth Sci. Rev., 89(1-2), 13–41, 2008.

Baker, M. B. and Peter, T.: Small-scale cloud processes and climate., Nature, 451(7176), 299–300, doi:10.1038/nature06594, 2008.

Broadley, S. L., Murray, B. J., Herbert, R. J., Atkinson, J. D., Dobbie, S., Malkin, T. L., Condliffe, E. and Neve, L.: Immersion mode heterogeneous ice nucleation by an illite rich powder representative of atmospheric mineral dust, Atmos. Chem. Phys., 12(1), 287–307, doi:10.5194/acp-12-287-2012, 2012.

Cantrell, W. and Heymsfield, A.: Production of Ice in Tropospheric Clouds: A Review, Bull. Am. Meteorol. Soc., 86(6), 795–807, doi:10.1175/BAMS-86-6-795, 2005.

Creamean, J. M., Suski, K. J., Rosenfeld, D., Cazorla, A., Demott, P. J., Sullivan, R. C., White, A. B., Ralph, F. M., Minnis, P., Comstock, J. M., Tomlinson, J. M. and Prather, K. A.: Dust and biological aerosols from the Sahara and Asia influence precipitation in the western U.S., Science, 339(6127), 1572–1578, doi:10.1126/science.1227279, 2013.

DeMott, P. J., Cziczo, D. J., Prenni, A. J., Murphy, D. M., Kreidenweis, S. M., Thomson, D. S., Borys, R. and Rogers, D. C.: Measurements of the concentration and composition of nuclei for cirrus formation, Proc. Natl. Acad. Sci. U. S. A., 100(25), 14655–14660, 2003.

DeMott, P. J., Prenni, A. J., Liu, X., Kreidenweis, S. M., Petters, M. D., Twohy, C. H., Richardson, M. S., Eidhammer, T. and Rogers, D. C.: Predicting global atmospheric ice nuclei distributions and their impacts on climate, Proc. Natl. Acad. Sci. U. S. A., 107(25), 11217–11222, 2010.

Eidhammer, T., DeMott, P. J. and Kreidenweis, S. M.: A comparison of heterogeneous ice nucleation parameterizations using a parcel model framework, J. Geophys. Res., 114, D06202, doi:10.1029/2008jd011095, 2009.

Ervens, B. and Feingold, G.: On the representation of immersion and condensation freezing in cloud models using different nucleation schemes, Atmos. Chem. Phys., 12, 5807–5826, doi:10.5194/acp-12-5807-2012, 2012.

Ervens, B. and Feingold, G.: Sensitivities of immersion freezing: Reconciling classical nucleation theory and deterministic expressions, Geophys. Res. Lett., 40(12), 3320–3324, doi:10.1002/grl.50580, 2013.

Ervens, B., Feingold, G., Sulia, K. and Harrington, J.: The impact of microphysical parameters, ice nucleation mode, and habit growth on the ice/liquid partitioning in mixed-phase Arctic clouds, J. Geophys. Res., 116(D17), D17205, doi:10.1029/2011JD015729, 2011.

Fletcher, N. H.: Active Sites and Ice Crystal Nucleation, J. Atmos. Sci., 26(6), 1266–1271, doi:10.1175/1520-0469(1969)026<1266:ASAICN>2.0.CO;2, 1969.

Fornea, A. P., Brooks, S. D., Dooley, J. B. and Saha, A.: Heterogeneous freezing of ice on atmospheric aerosols containing ash, soot, and soil, J. Geophys. Res., 114, D13201, doi:10.1029/2009JD011958, 2009.

Hiranuma, N., Augustin-Bauditz, S., Bingemer, H., Budke, C., Curtius, J., Danielczok, A., Diehl, K., Dreischmeier, K., Ebert, M., Frank, F., Hoffmann, N., Kandler, K., Kiselev, A., Koop, T., Leisner, T., Möhler, O., Nillius, B., Peckhaus, A., Rose, D., Weinbruch, S., Wex, H., Boose, Y., DeMott, P. J., Hader, J. D., Hill, T. C. J., Kanji, Z. A., Kulkarni, G., Levin, E. J. T., McCluskey, C. S., Murakami, M., Murray, B. J., Niedermeier, D., Petters, M. D., O'Sullivan, D., Saito, A., Schill, G. P., Tajiri, T., Tolbert, M. A., Welti, A., Whale, T. F., Wright, T. P. and Yamashita, K.: A comprehensive laboratory study on the immersion freezing behavior of illite NX particles: a comparison of 17 ice nucleation measurement techniques, Atmos. Chem. Phys., 15(5), 2489–2518, doi:10.5194/acp-15-2489-2015, 2015.

Hoose, C. and Möhler, O.: Heterogeneous ice nucleation on atmospheric aerosols: a review of results from laboratory experiments, Atmos. Chem. Phys., 12(20), 9817–9854, doi:10.5194/acp-12-9817-2012, 2012.

Hoose, C., Kristjánsson, J. E., Chen, J.-P. and Hazra, A.: A Classical-Theory-Based Parameterization of Heterogeneous Ice Nucleation by Mineral Dust, Soot, and Biological Particles in a Global Climate Model, J. Atmos. Sci., 67(8), 2483–2503, doi:10.1175/2010JAS3425.1, 2010.

Koehler, K. a., Kreidenweis, S. M., DeMott, P. J., Petters, M. D., Prenni, a. J. and Möhler, O.: Laboratory investigations of the impact of mineral dust aerosol on cold cloud formation, Atmos. Chem. Phys., 10(23), 11955–11968, doi:10.5194/acp-10-11955-2010, 2010.

Koop, T., Luo, B. P., Tsias, A. and Peter, T.: Water activity as the determinant for homogeneous ice nucleation in aqueous solutions, Nature, 406(6796), 611–614, 2000.

Liu, X. and Penner, J. E.: Ice nucleation parameterization for global models, Meteorol. Zeitschrift, 14(4), 499–514, 2005.

Lüönd, F., Stetzer, O., Welti, A. and Lohmann, U.: Experimental study on the ice nucleation ability of size-selected kaolinite particles in the immersion mode, J. Geophys. Res., 115(D14), 1–14, doi:10.1029/2009JD012959, 2010.

Marcolli, C., Gedamke, S., Peter, T. and Zobrist, B.: Efficiency of immersion mode ice nucleation on surrogates of mineral dust, Atmos. Chem. Phys., 7(19), 5081–5091, 2007.

Meyers, M. P., DeMott, P. J. and Cotton, W. R.: New primary ice-nucleation parameterizations in an explicit cloud model, J. Appl. Meteorol., 31(7), 708–721, 1992.

Mülmenstädt, J., Sourdeval, O., Delanoë, J. and Quaas, J.: Frequency of occurrence of rain from liquid-, mixed-, and ice-phase clouds derived from A-Train satellite retrievals, Geophys. Res. Lett., 42(15), 6502–6509, doi:10.1002/2015GL064604, 2015.

Murray, B. J., Broadley, S. L., Wilson, T. W., Atkinson, J. D. and Wills, R. H.: Heterogeneous freezing of water droplets containing kaolinite particles, Atmos. Chem. Phys., 11(9), 4191–4207, doi:10.5194/acp-11-4191-2011, 2011.

Murray, B. J., O'Sullivan, D., Atkinson, J. D. and Webb, M. E.: Ice nucleation by particles immersed in supercooled cloud droplets., Chem. Soc. Rev., 41(19), 6519–54, doi:10.1039/c2cs35200a, 2012.

Niedermeier, D., Shaw, R. a., Hartmann, S., Wex, H., Clauss, T., Voigtländer, J. and Stratmann, F.: Heterogeneous ice nucleation: exploring the transition from stochastic to singular freezing behavior, Atmos. Chem. Phys., 11(16), 8767–8775, doi:10.5194/acp-11-8767-2011, 2011.

Phillips, V. T. J., DeMott, P. J. and Andronache, C.: An Empirical Parameterization of Heterogeneous Ice Nucleation for Multiple Chemical Species of Aerosol, J. Atmos. Sci., 65(9), 2757–2783, doi:10.1175/2007JAS2546.1, 2008.

Phillips, V. T. J., Demott, P. J., Andronache, C., Pratt, K. A., Prather, K. A., Subramanian, R. and Twohy, C.: Improvements to an Empirical Parameterization of Heterogeneous Ice Nucleation and Its Comparison with Observations, J. Atmos. Sci., 70(2), 378–409, doi:10.1175/JAS-D-12-080.1, 2013.

Prather, K. A., Bertram, T. H., Grassian, V. H., Deane, G. B., Stokes, M. D., Demott, P. J., Aluwihare, L. I., Palenik, B. P., Azam, F., Seinfeld, J. H., Moffet, R. C., Molina, M. J., Cappa, C. D., Geiger, F. M., Roberts, G. C., Russell, L. M., Ault, A. P., Baltrusaitis, J., Collins, D. B., Corrigan, C. E., Cuadra-Rodriguez, L. A., Ebben, C. J., Forestieri, S. D., Guasco, T. L., Hersey, S. P., Kim, M. J., Lambert, W. F., Modini, R. L., Mui, W., Pedler, B. E., Ruppel, M. J., Ryder, O. S., Schoepp, N. G., Sullivan, R. C. and Zhao, D.: Bringing the ocean into the laboratory to probe the chemical complexity of sea spray aerosol., Proc. Natl. Acad. Sci. U. S. A., 110(19), 7550–5, doi:10.1073/pnas.1300262110, 2013.

Pruppacher, H. R. and Klett, J. D.: Microphysics of Clouds and Precipitation, edited by R. D. Rosen, Kluwer Academic Publishers., 1997.

Rosenfeld, D., Lohmann, U., Raga, G. B., O'Dowd, C. D., Kulmala, M., Fuzzi, S., Reissell, A. and Andreae, M. O.: Flood or drought: how do aerosols affect precipitation?, Science, 321(5894), 1309–13, doi:10.1126/science.1160606, 2008.

Sullivan, R. C., Miñambres, L., DeMott, P. J., Prenni, A. J., Carrico, C. M., Levin, E. J. T. and Kreidenweis, S. M.: Chemical processing does not always impair heterogeneous ice nucleation of mineral dust particles, Geophys. Res. Lett., 37(24), L24805, doi:10.1029/2010GL045540, 2010a.

Sullivan, R. C., Petters, M. D., DeMott, P. J., Kreidenweis, S. M., Wex, H., Niedermeier, D., Hartmann, S., Clauss, T., Stratmann, F., Reitz, P., Schneider, J. and Sierau, B.: Irreversible loss of ice nucleation active sites in mineral dust particles caused by sulphuric acid condensation, Atmos. Chem. Phys., 10, 11471–11487, 2010b.

Vali, G.: Freezing rate due to heterogeneous nucleation, J. Atmos. Sci., 51(13), 1843–1856, 1994.

Vali, G.: Repeatability and randomness in heterogeneous freezing nucleation, Atmos. Chem. Phys., 8(16), 5017–5031, 2008.

Vali, G.: Interpretation of freezing nucleation experiments: singular and stochastic; sites and surfaces, Atmos. Chem. Phys., 14(11), 5271–5294, doi:10.5194/acp-14-5271-2014, 2014.

Vali, G. and Stransbury, E. J.: Time Dependant Charactirisitcs of the Heterogeneous Nucleation of Ice, Can. J. Phys., 44(3), 477–502, 1966.

Vali, G., DeMott, P. J., Möhler, O. and Whale, T. F.: Technical Note: A proposal for ice nucleation terminology, Atmos. Chem. Phys., 15(18), 10263–10270, doi:10.5194/acp-15-10263-2015, 2015.

Welti, A., Lund, F., Stetzer, O. and Lohmann, U.: Influence of particle size on the ice nucleating ability of mineral dusts, Atmos. Chem. Phys., 9(18), 6705–6715, 2009.

Wex, H., Augustin-Bauditz, S., Boose, Y., Budke, C., Curtius, J., Diehl, K., Dreyer, A., Frank, F., Hartmann, S., Hiranuma, N., Jantsch, E., Kanji, Z. A., Kiselev, A., Koop, T., Möhler, O., Niedermeier, D., Nillius, B., Rösch, M., Rose, D., Schmidt, C., Steinke, I. and Stratmann, F.: Intercomparing different devices for the investigation of ice nucleating particles using Snomax® as test substance, Atmos. Chem. Phys., 15(3), 1463–1485, doi:10.5194/acp-15-1463-2015, 2015.

Wheeler, M. J. and Bertram, A. K.: Deposition nucleation on mineral dust particles: A case against classical nucleation theory with the assumption of a single contact angle, Atmos. Chem. Phys., 12(2), 1189–1201, doi:10.5194/acp-12-1189-2012, 2012.

Worringen, A., Kandler, K., Benker, N., Dirsch, T., Mertes, S., Schenk, L., Kästner, U., Frank, F., Nillius, B., Bundke, U., Rose, D., Curtius, J., Kupiszewski, P., Weingartner, E., Vochezer, P., Schneider, J., Schmidt, S., Weinbruch, S. and Ebert, M.: Single-particle characterization of ice-nucleating particles and ice particle residuals sampled by three different techniques, Atmos. Chem. Phys., 15(8), 4161–4178, doi:10.5194/acp-15-4161-2015, 2015.

Wright, T. P. and Petters, M. D.: The role of time in heterogeneous freezing nucleation, J. Geophys. Res. Atmos., 118(9), 3731–3743, doi:10.1002/jgrd.50365, 2013.

Wright, T. P., Petters, M. D., Hader, J. D., Morton, T. and Holder, A. L.: Minimal cooling rate dependence of ice nuclei activity in the immersion mode, J. Geophys. Res. Atmos., 118(18),

Atmos. Chem. Phys. Discuss., doi:10.5194/acp-2015-1013, 2016
Manuscript under review for journal Atmos. Chem. Phys.
Published: 18 January 2016

10,535–10,543, doi:10.1002/jgrd.50810, 2013.

Zobrist, B., Koop, T., Luo, B. P., Marcolli, C. and Peter, T.: Heterogeneous ice nucleation rate coefficient of water droplets coated by a nonadecanol monolayer, J. Phys. Chem. C, 111(1), 2149–2155, doi:10.1021/jp066080w, 2007.

Atmos. Chem. Phys. Discuss., doi:10.5194/acp-2015-1013, 2016
Manuscript under review for journal Atmos. Chem. Phys.
Published: 18 January 2016

Atmospheric Chemistry and Physics Discussions

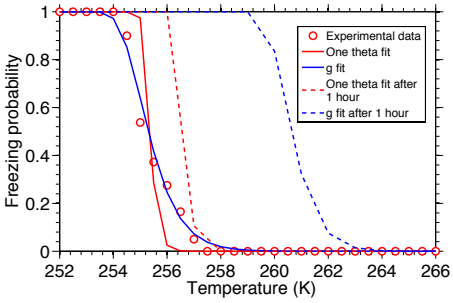

Figure 1. Experimentally determined freezing probabilities and fits from freezing of a droplet containing a single large ~300 μm diameter volcanic ash particle, from Fornea et al. (2009). Red dots are experimental freezing probabilities retrieved from repeated droplet freezing measurements. The red line is a fit to the data using classical nucleation theory and the assumption of a single contact angle (θ). The blue line is a fit to the data using the g framework developed here, which describes a Gaussian distribution of θ. The g fit has a least square error sum of 0.0197, $\mu = 1.65$, and $\sigma = 0.135$. The dotted red line is the simulated freezing curve resulting from a single θ distribution after the droplets are held at the same temperature for 1 hour. The dotted blue line is the freezing curve from a multiple θ distribution described by g after the same temperature hold simulation.

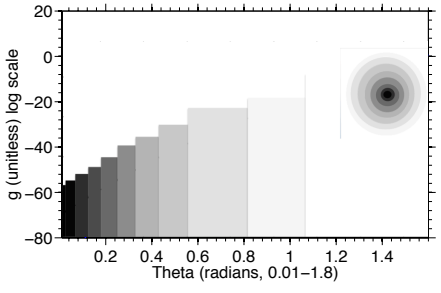

Figure 2. Upper right inset displays the distribution of ice nucleation activity (contact angle, θ) for a representative effective ice active surface site of an ice nucleating particle. The less active (white) surface sites have more surface coverage while the more active (black) surface sites have less coverage. The probability distribution function for a sample g distribution (mode = μ, standard deviation = σ) ascent in log space is plotted with numerical bins. The darker colors are used to highlight the stronger ice nucleating activity at smaller contact angles (θ).

Atmos. Chem. Phys. Discuss., doi:10.5194/acp-2015-1013, 2016
Manuscript under review for journal Atmos. Chem. Phys.
Published: 18 January 2016

Atmospheric Chemistry and Physics Discussions

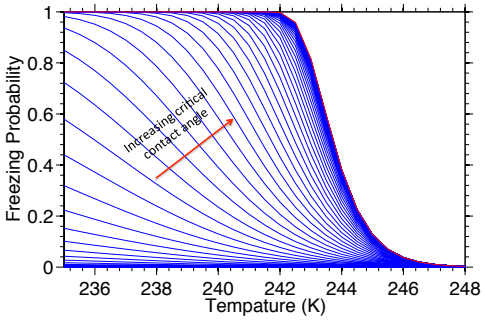

Figure 3. Identifying the critical contact angle range. The thin blue curves are retrieved from application of the simplified Eq. (10), which approximates the freezing probability by integrating over a smaller contact angle range, $[\theta_{c_1}, \theta_{c_2}]$, while the thick red curve is obtained from application of the complete Eq. (7), which integrates over the full contact angle range. Both approaches use the same sample g distribution.

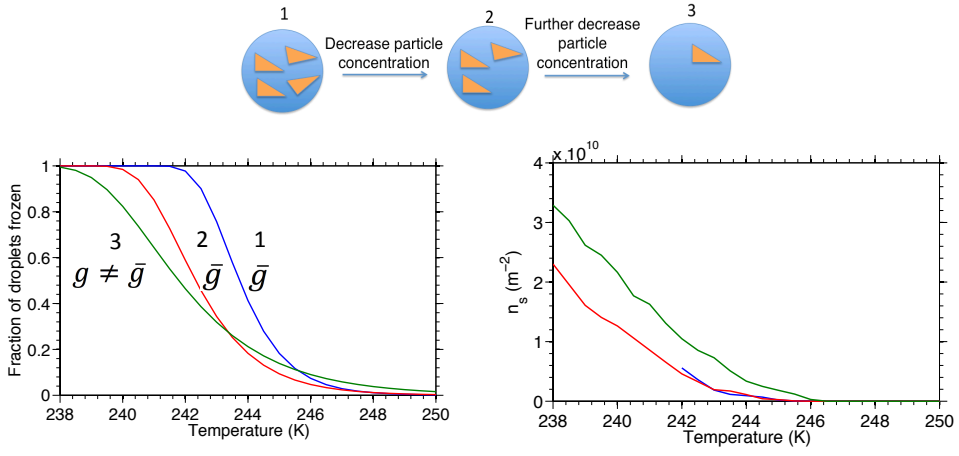

Figure 4. Top: Schematic summarizing the procedure for determining the critical area. **Left:** The frozen fraction freezing curves shift to lower temperatures initially due solely to the decrease in total surface area of the ice nucleating particles (curves 1 & 2). As the total surface area of the particles is decreased below the critical area threshold ($g \neq \bar{g}$) the slope of the freezing curve also broadens because the effective distribution of ice nucleating sites has changed – more external variability has been introduced (curve 3). **Right:** Ice active site density (n_s) retrieved from the frozen fraction plots on the left for the same three particle concentration systems. Above the critical area limit ($g = \bar{g}$) the two n_s curves are essentially the same, but below the critical area threshold ($g \neq \bar{g}$) n_s increases, even though the same particle species was measured in all three experiments. These exemplary frozen fraction and n_s curves were produced by fitting a $\bar{g}$ distribution to droplet freezing measurements of illite mineral particles from Broadley et al. (2012).

Atmos. Chem. Phys. Discuss., doi:10.5194/acp-2015-1013, 2016
Manuscript under review for journal Atmos. Chem. Phys.
Published: 18 January 2016

Atmospheric Chemistry and Physics Discussions

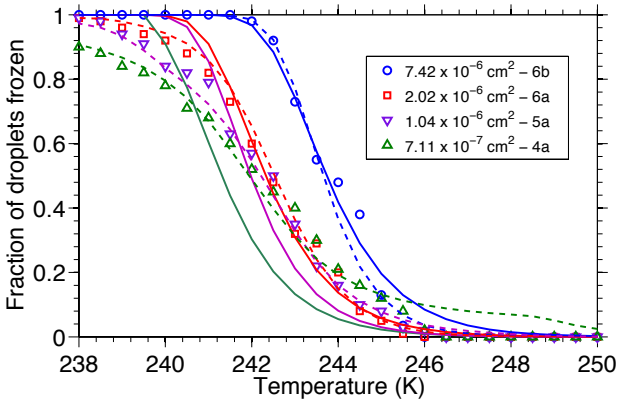

Figure 5. Experimental freezing curves for different surface area concentrations of illite mineral powder immersed in 10-20 μm diameter water droplets taken from Broadley et al. (2012) (circles). Lines are modeled predictions of the same data using the g distribution method. Solid lines are produced directly from the global $\bar{g}$ distribution first obtained from the high concentration system. The dashed lines are obtained by randomly sub-sampling the global $\bar{g}$ distribution as described in the text.

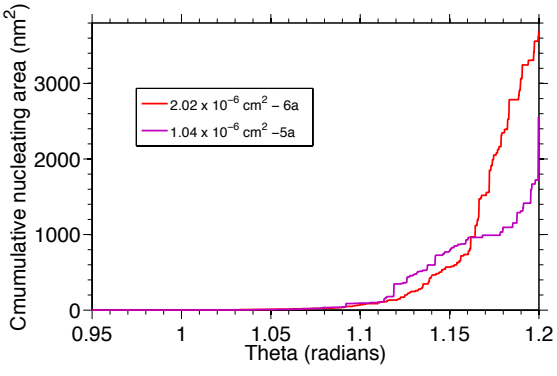

Figure 6. Cumulative ice nucleating surface areas from application of Eq. (11) to modeled average g distributions from systems 6a (red) and 5a (purple) in Fig. 5, taken from cold plate measurements of illite in droplets from Broadley et al. (2012), plotted against the critical contact angle range. At low contact angles the two systems have close total nucleating surface areas. This explains the similar onset of freezing before the eventual divergence at lower temperature (larger contact angle).